Cis–Trans Isomerization of [Pt(L-methionine)$_2$]: Metabolite of the Anticancer Drug Cisplatin

Piedad del Socorro Murdoch,[†] John D. Ranford,[†] Peter J. Sadler,*[,†] and Susan J. Berners-Price[‡]

Department of Chemistry, Birkbeck College, University of London, Gordon House and Christopher Ingold Laboratories, 29 Gordon Square, London WC1H OPP, U.K., and Division of Science and Technology, Griffith University, Nathan, Brisbane, Australia 4111

Received February 11, 1993

[Pt(L-Met-*S*,*N*)$_2$] is a metabolite of the anticancer drug *cis*-[PtCl$_2$(NH$_3$)$_2$] (cisplatin). We have discovered that it undergoes facile cis–trans isomerization in aqueous solution, and this has been investigated by reverse-phase HPLC, ^{1}H, ^{15}N, and 2D [^{1}H, ^{15}N] heteronuclear multiple quantum coherence (HMQC, using ^{15}N-labeled L-HMet) NMR, CD, and UV spectroscopy. The isomerization reactions are very slow (cis → trans k_{ct} 0.86 × 10^{-5} s^{-1}, trans → cis, k_{tc} 6.0 × 10^{-5} s^{-1}, 310 K), with the cis isomer predominating at equilibrium (K 7.0). The trans to cis isomerization appears to be entropy-driven. Molecular modeling and energy calculations (EHMO) for the three diastereomers of each geometrical isomer were carried out. The passage of the isomers through membranes and their excretion from the body are discussed in terms of the distribution of charge in the isomers and their hydration.

Introduction

Cisplatin, *cis*-[(PtCl$_2$(NH$_3$)$_2$], is a widely-used anticancer drug.[1] One of the few characterized metabolites of this drug is the L-methionine (L-HMet)[2] complex [(Pt(L-Met)$_2$] which has been isolated from urine.[3] Originally, this complex was assigned a trans configuration, but our recent NMR data[4] suggest that it exists in aqueous solution as a mixture of cis and trans isomers with the cis isomer predominating. Biological interest in L-HMet complexes such as this stems from the possibility that L-HMet enhances the nephrotoxicity of cisplatin.[5] However, L-HMet has been used as a rescue agent to remove excess Pt from the body,[6] and extracellular Pt(II)–L-Met complexes may be nontoxic[7,8] and readily excreted. Inside cells the formation of L-Met–Pt(II) complexes could provide an activation mechanism for cisplatin, e.g. in reactions with DNA, and we have noted[4] that one of the chelate rings of [(Pt(L-Met)$_2$] readily opens at acidic pH in the presence of chloride. No X-ray crystal structures of [(Pt(L-Met)$_2$] complexes have been reported. For each geometrical isomer, three diastereomers (*RR*, *RS*/*SR*, *SS*) exist due to the chirality of the coordinated sulfur. In addition, the conformation of the 6-membered S,N chelate ring is dependent on the chirality of the coordinated sulfur. In the crystal structure[9] of [PtCl$_2$(L-Met-*S*,*N*)], both *R* and *S* diastereomers have chair-like ring conformations, whereas, in aqueous solution, NMR ^{1}H–^{1}H coupling constants suggest that the conformations of the rings differ.[4]

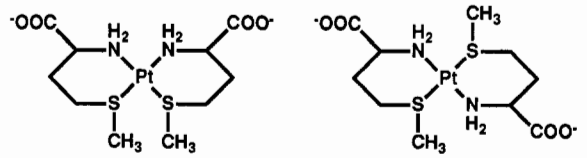

There are very few previous detailed studies of the isomerization of other Pt(II) complexes in aqueous solution.[10] The majority of isomerization studies have been carried out in nonprotic solvents with alkyl and phosphine Pt(II) complexes and the trans isomer is often thermodynamically favored.[11–15] A range of mechanisms has been proposed for cis–trans isomerizations including dissociation to give a three-center transition state, association to give a five-coordinate intermediate, and involvement of tetrahedral intermediates.[16]

In this paper we report the separation of the cis and trans isomers of [(Pt(L-Met-*S*,*N*)$_2$] using HPLC, and detailed studies of isomerization reactions in aqueous solution using multinuclear NMR, UV, and CD spectroscopy. In particular we use [^{1}H, ^{15}N] heteronuclear multiple quantum coherence (HMQC) NMR spectroscopy[17] for the rapid detection of both ^{15}N and ^{1}H resonances of NH$_2$ groups of bound [^{15}N]-L-Met. Energy calculations and molecular modeling were also carried out to provide insight into the relative stabilities of, and charge

[†] Birkbeck College, University of London.
[‡] Griffith University.

(1) (a) *Platinum and Other Metal Complexes in Cancer Chemotherapy*; Nicolini, M., Ed.; Martinus Nijhoff: Boston, MA, 1988. (b) *Platinum and Other Metal Complexes in Cancer Chemotherapy*; Howell, S. B., Ed.; Plenum Press: New York, 1991.
(2) Abbreviations used are as follows: L-methionine, L-HMet; extended Hückel molecular orbital, EHMO; high pressure (performance) liquid chromatography, HPLC; circular dichroism, CD; heteronuclear multiple quantum coherence, HMQC.
(3) (a) Repta, A. J.; Long, D. F. In *Cisplatin; Current Status and New Developments*; Prestayko, A. W., Crooke, S. T., Carter, S. K., Eds.; Academic Press: New York, 1980; pp 285–304. (b) Riley, C. M.; Sternson, L. A.; Repta, A. J.; Slyter, S. A. *Anal. Biochem.* **1983**, *130*, 203–214. (c) Sternson, L. A.; Repta, A. J.; Shih, H.; Himmelstein, K. J.; Patton, T. F. In *Platinum Coordination Complexes in Cancer Chemotherapy*; Hacker, M. P., Douple, E. B., Krakhoff, I. H., Eds.; Martinus Nijhoff: Boston, MA, 1984; pp 126–137.
(4) Norman, R. E.; Ranford, J. D.; Sadler, P. J. *Inorg. Chem.* **1992**, *31*, 877–888.
(5) Alden, W. W.; Repta, A. J. *Chem. Biol. Interact.* **1984**, *48*, 121–126.
(6) Melvik, J. E.; Pettersen, E. O. *Inorg. Chim. Acta* **1987**, *137*, 115–118.
(7) Andrews, P. A.; Wung, W. E.; Howell, S. B. *Anal. Biochem.* **1984**, *143*, 46–56.
(8) Daley-Yates, P. T.; McBrien, D. C. *Biochem. Pharm.* **1984**, *33*, 3063–3070.
(9) (a) Freeman, H. C.; Golomb, M. L. *J. Chem. Soc., Chem. Commun.* **1970**, 1523–1524. (b) Wilson, C.; Scudder, M. L.; Hambley, T. W.; Freeman, H. C. *Acta Crystallogr.* **1992**, *C48*, 1012–1015.
(10) Scandola, F.; Traverso, O.; Balzani, V.; Zucchini, G. L.; Carassiti, V. *Inorg. Chim. Acta* **1967**, *1*, 76–80.
(11) (a) Kelm, H.; Louw, W. J.; Palmer, D. A. *Inorg. Chem.* **1980**, *19*, 843–847. (b) MacDougall, J. J.; Nelson, J. H.; Mathey, F. *Inorg. Chem.* **1982**, *21*, 2145–2153. (c) Romeo, R.; Minniti, D.; Lanza, S. *Inorg. Chem.* **1980**, *19*, 3663–3668.
(12) Price, J. H.; Birk, J. P.; Wayland, B. B. *Inorg. Chem.* **1978**, *8*, 2245–2250.
(13) Alibrandi, G.; Cusumano, M.; Minniti, D.; Scolaro, L. M.; Romeo, R. *Inorg. Chem.* **1989**, *28*, 342–347.
(14) Alibrandi, G.; Minniti, D.; Scolaro, L. M.; Romeo, R. *Inorg. Chem.* **1988**, *27*, 318–324.
(15) Belluco, U. *Organometallic and Coordination Chemistry of Platinum*; Academic Press: London, 1974; pp 81–84.
(16) Wilkins, R. G. *Kinetics and Mechanism of Reactions of Transition Metal Complexes*, 2nd ed.; VCH: Weinheim, Germany, 1991; pp 356–359.
(17) Bax, A.; Griffey, R. H.; Hawkins, B. L. *J. Magn. Reson.* **1983**, *55*, 301–5.

0020-1669/93/1332-2249$04.00/0

distributions within, the various isomers of [(Pt(L-Met-*S*,*N*)$_2$], and the relevance of these to their biological properties is discussed.

Experimental Section

Materials. L-Methionine (L-HMet)[2] was purchased from Sigma, [^{15}N]-L-methionine (99 atom % ^{15}N) from MSD Isotopes, $K_2[PtCl_4]$, and *cis*-$[PtCl_2(NH_3)_2]$ from Johnson Matthey plc, and *cis*-$[PtCl_2(^{15}NH_3)_2]$ was synthesized as previously described.[18] HPLC grade methanol and all other chemicals were purchased from Aldrich. HPLC solvent filters (0.2 μm) were obtained from Millipore.

NMR. NMR spectra were recorded on the following instruments: JEOL GSX500 (^{1}H 500 MHz, ^{15}N 50.70 MHz), JEOL GSX270 (^{15}N 27.38 MHz), Bruker AM400 (^{1}H 400 MHz), and Bruker AM500 (^{1}H 500 MHz, ^{15}N 50.70 MHz) using 5-mm NMR tubes. The chemical shift references were as follows: ^{1}H, TSP; ^{15}N, 1.5 M $^{15}NH_4Cl$ in 1 M HCl containing 10% D_2O. For ^{1}H NMR, typical acquisition conditions for 1D spectra were 45–60° pulses, 32K data points, 2–3-s relaxation delay, and collection of 64–128 transients, giving a final digital resolution of 0.19 Hz/point. The residual HOD signal was suppressed by continual or gated secondary irradiation. Exponential or Gaussian functions were applied to free induction decays prior to transformation, as required. ^{195}Pt satellites of ^{1}H resonances were too broad to detect at these field strengths due to relaxation via chemical shift anisotropy.[19] Standard programs were used to acquire phase-sensitive 2D COSY spectra.

^{15}N-edited ^{1}H NMR spectra and [^{1}H–^{15}N] HMQC NMR spectra were recorded on the Bruker AM500 spectrometer fitted with a BSV-7 transmitter, a BFX-5 X nucleus decoupler, and a 5-mm inverse probehead as we have reported previously,[20] with sequences optimized for $J(^1H, ^{15}N)$ = 73 Hz. For HMQC NMR experiments, samples of lyophilized *cis*- and *trans*-[Pt(L-Met-*S*,*N*)$_2$] were dissolved in 0.5 mL of 5% D_2O/95% H_2O, and 30 μL of phosphate buffer (100 mM, pH 7.0) was added, giving a phosphate concentration of 5.6 mM. Spectra were recorded soon after dissolution, at a probe temperature of 283 K. The pH values of the NMR solutions were 7.18 for *cis*-[Pt(L-Met-*S*,*N*)$_2$] and 7.53 for the trans isomer. Lyophilized samples have been stored for several months at ambient temperature without any indication of isomerization.

HPLC. The following equipment was used: Gilson 305 pumps, Gilson 806 manometric module, LKB 2141 variable wavelength monitor, LKB 2221 integrator, and Rheodyn sample injector. For analytical work, two C18 reverse-phase columns were used: a lichrosorb 5PR18 (25 cm × 4.6 mm, 5 μm, Technicol), and a dynamax microsorb (10 cm × 4.6 mm, 3 μm, Rainin Instrument Company). Preparative work was carried out on a dynamax microsorb C18 reverse-phase column (25 cm × 21.4 mm, 5 μm, Rainin Instrument Company). Samples were run isocratically with H_2O or 95% H_2O/5% methanol (lichrosorb column) as the eluant. Higher concentrations of methanol resulted in faster elution but reduced resolution. Elution with phosphate buffer (0.1 M, pH 7) gave slightly increased resolution, with only minor changes in the retention times, but this and organic solvents, e.g. CH_3CN, were not used routinely due to the possibility of ligand substitution reactions with the complexes being separated.[21]

CD and UV. CD spectra were recorded on a JASCO J-600 spectropolarimeter equipped with an IBM computer interface (University of London Intercollegiate Research Service, Birkbeck College), using 0.5-mm pathlength cells and 0.67 mM solutions of HPLC isolates. UV spectra were obtained on a Varian 2390 spectrophotometer using 1- and 0.05-cm pathlength cells.

Mass Spectra. Spectra were obtained from HPLC isolates using the FAB method (University of London Intercollegiate Research Service, School of Pharmacy), with *m*-nitrobenzyl alcohol as the matrix.

Molecular Modeling and EHMO Calculations. Initial molecular models of the diastereomers of *cis*- and *trans*-[Pt(L-Met-*S*,*N*)$_2$] were based on the X-ray crystallographic coordinates of [$PtCl_2$(L-HMet)].[9] The chloride ligands in the latter structure were substituted by a second L-Met with *trans*-N–Pt–N and -N–Pt–S angles of 180°. Modeling and energy minimization was carried out on a Silicon Graphics Personal Iris 4D35TG computer using Polygen Quanta (3.2.4) in the CHARMm force-field. For this, the PtN_2S_2 coordination sphere was constrained and initial structures were chosen with the carboxylate group quasi-equatorial. Energy calculations were performed on a SUN SPARC 2 computer with a version of Hoffmann's program supplied by Dr. R. Deeth (University of Bath). This implemented the standard EHMO method as previously described.[22] Standard parameters were used for Pt and the other atoms. Dipole moments were calculated using the standard Quanta program, with the partial charges calculated by the EHMO method.

Kinetics. Kinetic parameters were fitted to the rate data using the Apple Macintosh package Kaleidagraph (Sinergy Software, Reading, PA).

HPLC Samples. Time Course of Reactions. The time course reaction between $K_2[PtCl_4]$ (20.75 mg, 10.0 mmol) in H_2O (5 mL) and L-HMet (14.80 mg, 19.8 mmol) at 296 K was followed chromatographically by injection of aliquots of the mixture (pH 2.5) onto the HPLC column at various time intervals. After 4 h of reaction no further change was observed in the chromatograms. The procedure was repeated after adjustment of the initial pH to 8.0 (with 0.33 M KOH) immediately after mixing.

Equilibrium Solutions of [Pt(L-Met-*S*,*N*)$_2$]. L-HMet (39.4 mg, 0.26 mmol) and $K_2[PtCl_4]$ (55.5 mg, 0.13 mmol) were heated to 353 K in water (4 mL) for 5 min. The pH of this was then raised from 2.4 to 7.0 (with 0.33 M KOH) during which time the initial faint yellow-colored solution became colorless. The volume was made up to 5 mL with H_2O to give a Pt concentration of 26 mM. This solution was then filtered through a 0.2-μm filter prior to HPLC injection. Similar HPLC traces were obtained after reaction of *cis*-$[PtCl_2(NH_3)_2]$ (40.2 mg, 0.13 mmol) with L-HMet (39.7 mg, 0.26 mmol) in water (4 mL) after heating at 353 K for 30 min with stirring. In the latter case the pH of the colorless solution was raised from 4.4 to 7.0, and the volume again made up to 5 mL. UV spectra were recorded for all reactants and equilibrium solutions, and 210 nm was chosen to monitor HPLC elution. Fractions from preparative HPLC runs were collected and immediately frozen.

Results

In this paper we have studied the reactions between $K_2[PtCl_4]$ and L-HMet in a 1:2 mol ratio. The major products (isomers of [Pt(L-Met)$_2$]) have been separated by HPLC, and further characterized using HPLC, multinuclear 1D (^{1}H and ^{15}N) and 2D [^{1}H–^{15}N] HMQC and COSY NMR methods, and mass, CD, and electronic absorption spectroscopies. The same species are also formed on reaction of cisplatin with L-HMet in a 1:2 ratio. The kinetics of cis–trans isomerization reactions of [Pt(L-Met)$_2$] have been investigated and EHMO calculations have been carried out on the modeled isomers.

HPLC. The time courses of reactions of $[PtCl_4]^{2-}$ and L-HMet (1:2, 296 K) at pH 2.5 or 8.0 were followed by HPLC using a reverse phase, C18 column eluted with 95% H_2O/5% MeOH. Three peaks, labeled **dv** (dead volume), **b**, and **c** (retention times 1.0, 2.1, and 2.8 min, respectively) were initially observed. After 10 min, peak **b** had almost disappeared and peak **dv** had decreased in intensity to a constant value of 0.5% of the total integrated intensity whereas **c** had concomitantly increased in intensity. Peaks **dv** and **b** were assigned to $[PtCl_4]^{2-}$/solvent front and L-HMet respectively via comparisons with chromatograms of these compounds alone, and via spiking experiments. After 20 min of reaction time, a new peak **t** was detected (retention time 1.6 min), and subsequently increased in intensity at the expense of peak **c** and attained equilibrium after 24 h (**c**:**t** ratio, 98:2, 20 min; 96:4, 70 min; 91:9, 4.4 h; 24 h, 87:13). When fractions corresponding to peaks **c** and **t** were collected from a preparative C18 column and were rechromatographed on an analytical column, initially only a single corresponding peak was seen. However, with time the peak for the other component (**c** or **t**) appeared, Figure 1, and increased in concentration until eventually the original 87:13 **c**:**t** equilibrium ratio was reestablished. Subsequent experiments (vide infra) allowed assignment of peaks **c** and **t** to the cis and trans isomers of [Pt(L-Met)$_2$], respectively. Chromatographing the starting solution at pH 2 (using HNO_3 to lower the pH) did not alter the elution profile.

Plots of the time dependence of peaks **c** and **t**, Figure 2, obtained by integration of the chromatograms, followed pseudo-first-order kinetics and allowed the rate constants for cis → trans (k_{ct}) and

(18) Kerrison, S. J. S.; Sadler, P. J. *J. Chem. Soc., Chem. Commun.* **1977**, 861–863.
(19) Ismail, I. M.; Kerrison, S. J. S.; Sadler, P. J. *Polyhedron* **1982**, *1*, 57–59.
(20) (a) Berners-Price, S. J.; Frenkiel, T. A.; Frey, U.; Ranford, J. D.; Sadler, P. J. *J. Chem. Soc., Chem. Commun.* **1992**, 789–791. (b) Berners-Price, S. J.; Frenkiel, T. A.; Ranford, J. D.; Sadler, P. J. *J. Chem. Soc., Dalton Trans.* **1992**, 2137–2139.
(21) Riley, C. M.; Sternson, L. A.; Repta, A. J. *Anal. Biochem.* **1982**, *124*, 167–179.
(22) Curtis, M. D.; Eisenstein, O. *Organometallics* **1984**, *3*, 887.

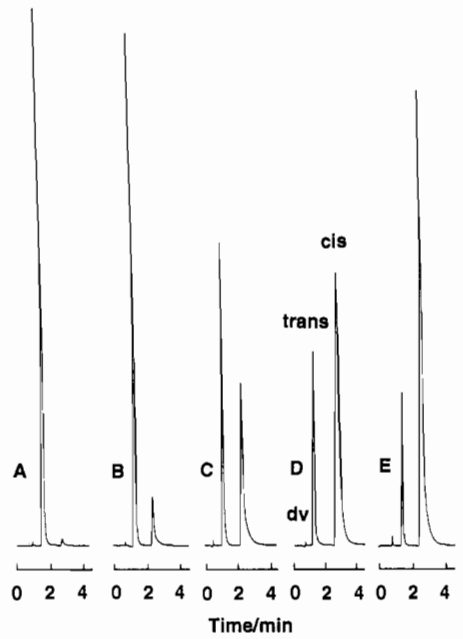

Figure 1. HPLC chromatograms (absorbance at 210 nm versus retention time) of an aqueous solution of *trans*-[Pt(L-Met-*S*,*N*)$_2$] at various times after incubation at 296 K: (A) 10 min; (B) 190 min; (C) 24 h; (D) 49 h; (E) 240 h (equilibrium) (**dv** = dead volume).

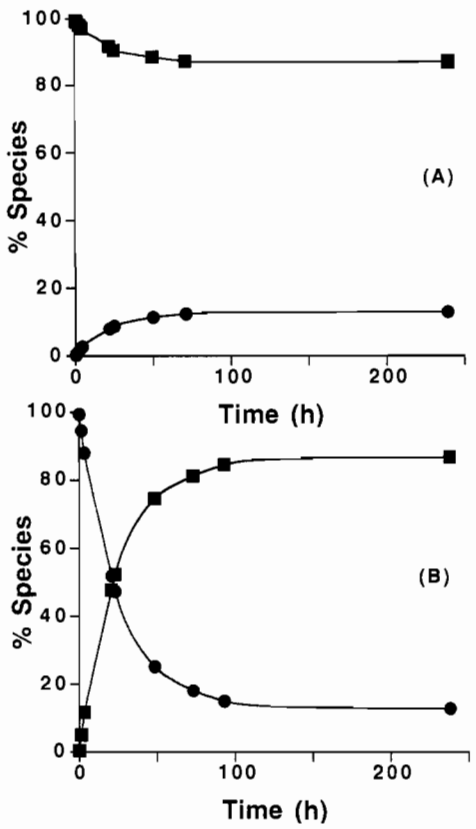

Figure 2. Plots of the isomerization of isolated (A) *cis*-[Pt(L-Met-*S*,*N*)$_2$] (■) and (B) *trans*-[Pt(L-Met-*S*,*N*)$_2$] (●) at 296 K as determined by HPLC. The solid curves are computer generated best fits using the rate constants given in Table I.

trans → cis (k_{tc}) isomerizations to be determined. This gave values of 1.2×10^{-5} s^{-1} for k_{tc} and 1.8×10^{-6} s^{-1} for k_{ct} (half-lives of 16.0 and 107 h for the trans and cis isomers respectively) at 296 K, Table I. At body temperature (310 K) the corresponding half-lives are 3.2 and 22.4 h. An Arrhenius plot (ln k vs $1/T$) gave E_a values of 95.7 kJ mol^{-1} for cis to trans isomerization and 97.7 kJ mol^{-1} for trans to cis isomerization. Changing the pH of the reequilibrium solutions from 7.0 to 3.9 did not alter the rate constants, and the rates of isomerization were also unaffected

Table I. Kinetic Data for the Isomerization of [Pt(L-Met-*S*,*N*)$_2$]

Rate Constants			
T/K	$10^4 k_{tc}$/s^{-1}	$10^4 k_{ct}$/s^{-1}	K^a
296.0	0.12	0.018	6.7[b]
303.0	0.29	0.042	6.9
310.0	0.60	0.086	7.0
318.0	1.5	0.22	6.8
328.0	6.2	0.84	7.4

Activation Parameters (296 K)			
	$\Delta G^{\ddagger}$/kJ mol^{-1}	$\Delta H^{\ddagger}$/kJ mol^{-1}	$\Delta S^{\ddagger}$/J mol^{-1} K^{-1}
trans → cis	101	95 ± 6	−18 ± 16
cis → trans	105	93 ± 5	−41 ± 16

[a] Equilibrium constant $K = k_{tc}/k_{ct}$ = [cis]/[trans]. [b] trans → cis: $\Delta G°$ −4.7 kJ mol^{-1}; $\Delta H°$ 2.1 kJ mol^{-1}; $\Delta S°$ 23 J mol^{-1} K^{-1}.

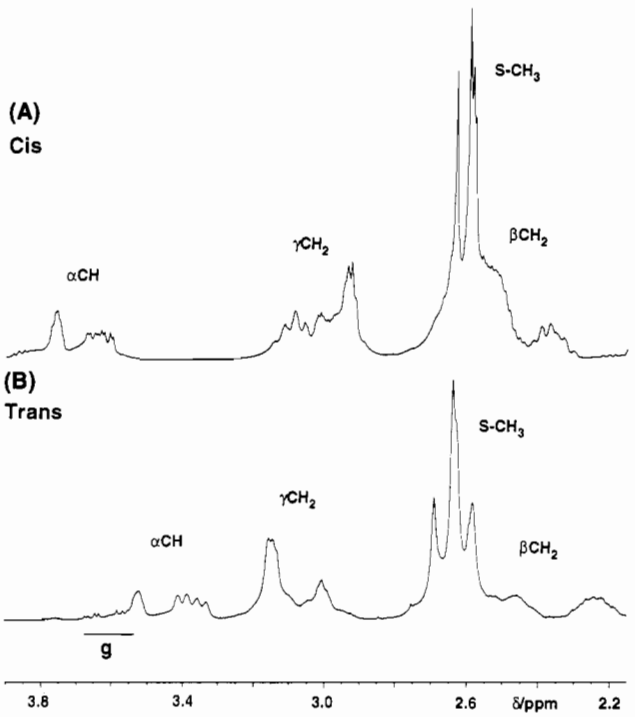

Figure 3. 400-MHz ^{1}H NMR spectra of *cis*-[Pt(L-Met-*S*,*N*)$_2$] (A), and *trans*-[Pt(L-Met-*S*,*N*)$_2$] (B) at 296 K. The peaks for the diastereomers of the *trans* isomer are notably broader than those for the cis isomer, probably due to chemical exchange processes. For detailed assignments see Table II (g = glycerol impurity).

by a 5-fold dilution of either isomer. Further kinetic data (Table I) were obtained by monitoring the isomerization by electronic absorption spectroscopy (225 nm, vide infra) at various temperatures.

NMR. ^{1}H NMR spectra of samples corresponding to peak **c** (lyophilized and redissolved in D_2O) contained four CH_3 singlets from 2.58 to 2.64 ppm and four αCH doublet of doublets between 3.61 and 3.76 ppm, along with βCH_2 multiplets between 2.35 and 2.59 ppm, and γCH_2 multiplets between 2.93 and 3.12 ppm, Figure 3A and Table II. A ^{1}H 2D phase-sensitive DQF-COSY spectrum in D_2O allowed assignments to be made for four sets of methionine resonances. The methyl peaks could not be simply correlated with those of the other protons, so their assignments are based on a consideration of relative intensities together with previous tentative assignments[4] from the reaction of L-HMet with cisplatin (1:1). The αCH resonances form two pairs at 3.613 and 3.652 ppm, and 3.752 and 3.760 ppm with the approximate relative intensities of 1.7:1.2:1.0:1.2, respectively, giving a 4:3 ratio for the pairs of resonances at 3.6 and 3.7 ppm. The $^3J(\alpha CH-\beta_a CH_2)$ values differ between the pairs of species, those for the resonances at 3.6 ppm being ca. 9.5 Hz and those for the peaks at 3.7 ppm being ca. 7 Hz. All $^3J(\alpha CH-\beta_b CH_2)$ couplings were

Table II. NMR Chemical Shifts, Coupling Constants, and Calculated Dipole Moments for the Isomers of $[Pt(L\text{-Met})_2]^a$

	$\delta(^1H)$								$^3J(^1H-^1H)$/Hz					
	αCH	$\beta_a CH_2$	$\beta_b CH_2$	$\gamma_a CH_2$	$\gamma_b CH_2$	NH_a	NH_b	CH_3	α-β_a	α-β_b	α-NH_a	α-NH_b	$\delta(^{15}N)$	dipole moment, D
cis-RR	3.613	2.350	2.574	3.002	3.087	5.49	5.65	2.631	9.7	3.5	9.0	<2	−20.65	27.6
cis-RS	3.652	2.371	2.546	2.993	3.116	5.44	5.79	2.580	9.1	3.3	9.0	<2	−20.71	29.4
cis-$\overline{RS}$	3.760	2.458	2.540	2.93	2.93	5.49	5.77	2.595	7.0	4.0	4.8	<2	−21.69	
cis-SS	3.752	2.486	2.587	2.93	2.93	5.38	5.69	2.586	7.0	3.3	4.0	<2	−21.78	29.1
trans-RR	3.343	*b*				*c*		2.691	11.0	1.7			−42.9	8.7
trans-RS	3.401							2.584	10.6	2.9			−39.7[d]	11.9
trans-$\overline{RS}$	3.525							2.639	4.6	4.6			−39.7	
trans-SS	3.522							2.632	4.2	4.2			−39.7	10.5

[a] The assignment of peaks to individual diastereomers is arbitrary, except that calculated ring conformations were used as a guide to assignment of ^1H NMR peaks via coupling constant analyses. The pairing of these with methyl and NH peaks was on the basis of peak intensities where possible. This procedure was more difficult to follow for the trans isomers because of broadening of ^1H NMR peaks; arbitrarily the αCH resonance of the trans isomers have been given a chemical shift ordering similar to that for the cis isomers. [b] Resonances too broad to analyze, see Figure 3B. [c] $^2J(NH_a-NH_b)$ values ca. 12 Hz; αNH peaks not analyzed in detail for the trans isomer (see Figure 4B); δ values 5.2–5.6 ppm; several $^3J(\alpha CH-NH)$ values appear to be 9–14 Hz. [d] Assumed to be three overlapping peaks.

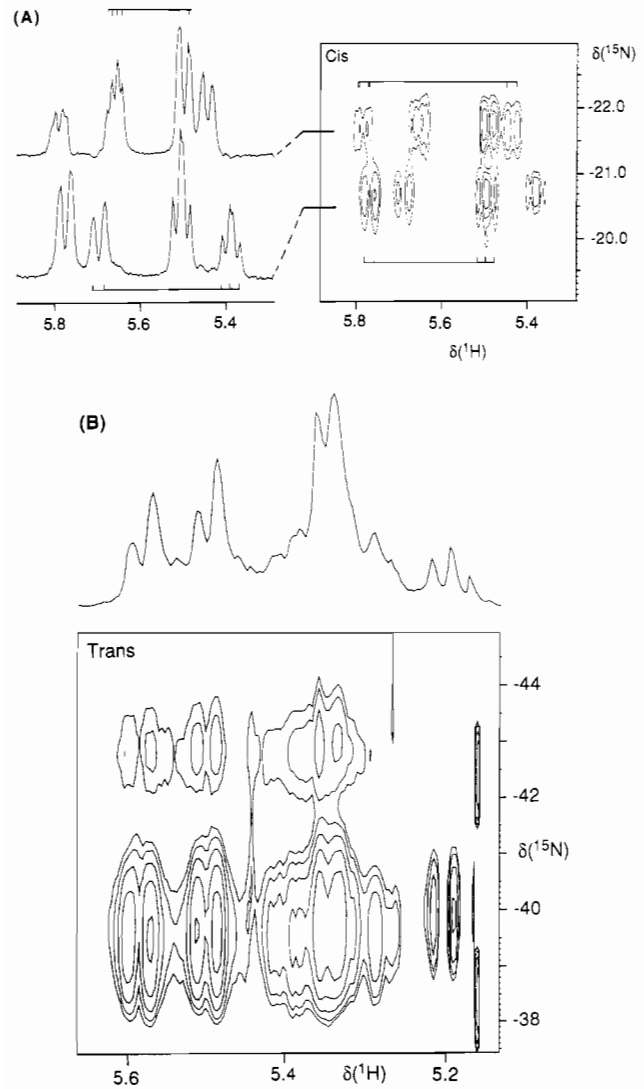

Figure 4. 2D $[^1H, ^{15}N]$ HMQC spectra of (A) *cis*-$[Pt(L\text{-Met-}S,N)_2]$ and (B) *trans*-$[Pt(L\text{-Met-}S,N)_2]$ at 283 K. For the cis isomer, two slices are shown each of which contains two pairs of NH proton resonances corresponding to ^{15}N shifts in *RR* or *RS* and in *SS* or *SR* diastereomers. Each multiplet contains $^2J(NH_a-NH_b)$ and $^3J(NH-\alpha CH)$ couplings. Peaks for the trans isomer are broader, and $^1H-^1H$ couplings are not clearly resolved, but two different ^{15}N shifts are apparent. An ^{15}N-edited ^1H NMR spectrum for the trans isomer is also shown. Chemical shifts and couplings are given in Table II.

similar, 3.3–4.0 Hz. The $^3J(\alpha CH-NH_2)$ values determined from HMQC experiments, Figure 4, also showed a pairing pattern with all αCH-NH_b values <2 Hz, but now the high-frequency pair has the smaller $^3J(\alpha CH-NH_a)$ of ca. 4.5 Hz; cf. 9.0 Hz for the low-frequency set.

When the probe temperature was progressively raised from 296 to 348 K, all signals initially broadened with loss of fine structure. The methyl singlets at 2.580 and 2.586 ppm coalesced at ca. 308 K, and upon further heating this peak coalesced with the signal originally at 2.595 ppm. By 338 K, all four CH_3 resonances had collapsed into one peak which continued to sharpen with increasing temperature. The αCH resonances broadened rapidly on raising the temperature, and at 348 K the two pairs of signals appeared to have just coalesced.

The isolated sample corresponding to the HPLC peak **t** also gave rise to four sets of signals but there is broadening of the spectrum at 296 K, which is most notable for the αCH resonances, Figure 3B. Cooling the sample to 278 K sharpened the spectrum sufficiently to allow resolution of $^3J(\alpha CH-\beta CH_2)$ couplings. The general pattern of the resonances is similar to that of the **c** sample, with two sets of two αCH signals, the low frequency pair of which has the larger associated couplings. The high frequency pair now appear as triplets with couplings of 4.2 and 4.6 Hz. The resonances for the α and β protons for sample **t** have shifts to lower frequency of those for sample **c**, whereas those for the γ protons are to higher frequency.

DEPT ^{15}N NMR spectra of a ^{15}N-labeled sample **c** (20 mM, 0.1 M pH 7 phosphate buffer, 296 K) showed four signals in two pairs at −20.65, −20.71, −21.69, and −21.78 ppm, Table II. The corresponding spectrum of ^{15}N-labeled sample **t** obtained under similar conditions exhibited one strong resonance at −39.7 ppm, along with a weaker signal at −42.9 ppm. These observations of ^{15}N NMR peaks were confirmed by 2D HMQC NMR spectra (Figure 4).

CD and UV Spectra. The UV spectrum of sample **c** at pH 7 has two resolved strong absorption bands at 204 and 255 nm (ϵ 12 700 and 1000 M^{-1} cm^{-1}, respectively) accompanied by a much weaker band at 300 nm (ϵ 45 M^{-1} cm^{-1}), Figure 5C and Table III. The spectrum of sample **t** is similar, with peaks at 206 and 255 nm (ϵ 11 300 and 1000 M^{-1} cm^{-1}, respectively) and 300 nm (ϵ 40 M^{-1} cm^{-1}) except that a pronounced shoulder is also seen at 220 nm. The CD spectra of the two complexes display the same general pattern of positive and negative bands, Figure 5A, although now there are more significant differences between them. Whereas sample **c** has one negative band resolved at 228 nm, sample **t** has two at 218 and 232 nm resulting in a very distinctive spectrum for each. After heating solutions of samples **c** and **t** at 310 K for 1 week, they gave rise to identical CD spectra, Figure 5(B). It was possible to simulate the spectrum of these equilibrium solutions by addition of spectra of the individual components **c** and **t** in a ratio of 87:13.

Mass Spectra. The parent molecular ions of HPLC samples **c** and **t** had the same isotopic abundance pattern, corresponding to one Pt per molecule, with the most intense peak at 492 amu

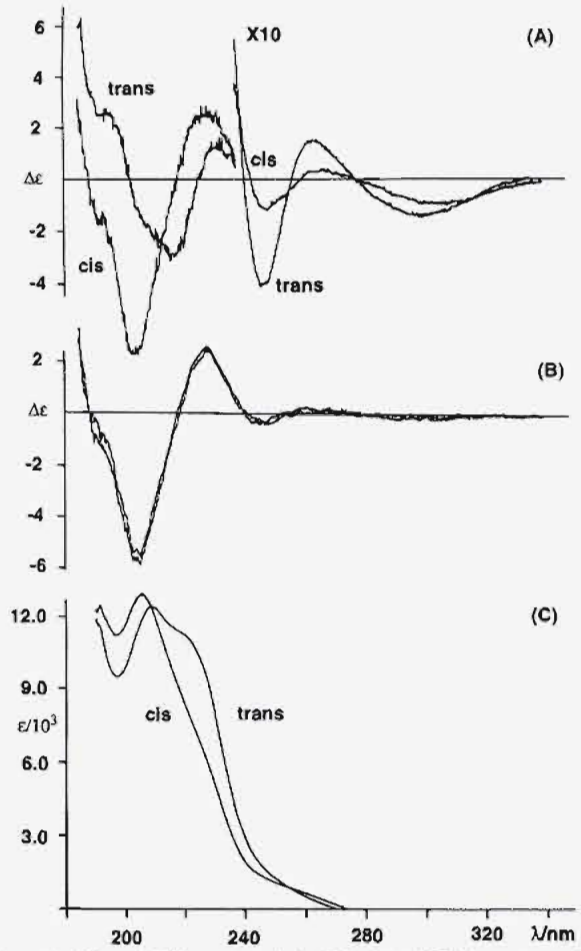

Figure 5. CD and UV spectra of *cis*-[Pt(L-Met-*S*,*N*)$_2$] and *trans*-[Pt(L-Met-*S*,*N*)$_2$] in H_2O: (A) CD spectra of isolated isomers; (B) CD spectra of solutions used for part A after equilibration (2 weeks); (C) UV spectra of isolated isomers.

Table III. UV and CD Data for the Cis and Trans Isomers of [Pt(L-Met-*S*,*N*)$_2$] in Aqueous Solution

method	λ (nm)			
	Cis Complex			
UV[a]	204 (12 700)		255 (1000)	300 (45)
CD[b]	192 (−1.7)	228 (+2.5)	247 (−0.40)	300 (−0.15)
	204 (−6.8)		263 (+0.15)	
	Trans Complex			
UV[a]	206 (11 300)	220 (sh)	255 (1000)	300 (40)
CD[b]	195 (+2.5)	218 (−3.0)	248 (−0.12)	305 (−0.09)
	207 (−2.0)	232 (+1.2)	266 (+0.04)	

[a] ε (M^{-1} cm^{-1}) in brackets. [b] Δε (M^{-1} cm^{-1}) in brackets.

(M + 1, M = [Pt(L-Met)$_2$]). In addition there were peaks for fragments at 447 (M − CO_2), 432 (M − CO_2 − CH_3), and 344 amu (M − (L-Met)), all with the characteristic Pt isotope pattern.

EHMO Calculations. Energy-minimized structures for the six diastereomers are shown in Figure 6. Two space-filling model energy-minimizied structures are shown in Figure 7. The calculated energies of the three diastereomers of the cis isomer were all lower than those calculated for the three trans diastereomers, with an average energy difference of 42 kJ mol^{-1}. The calculated charge distribution was almost the same for the diastereomers of each geometrical isomer, but there were significant differences between the cis and trans isomers: notably the higher partial charge (+1.73) on Pt in the cis isomer compared to the trans (+1.15), and greater negative charge (−0.54) on the coordinated S atoms of the cis isomer compared to the trans (−0.35). Consequently the cis isomer is distinctly more polar than the trans isomer, with negatively-charged carboxylates and nitrogens on one side of the molecule and the negatively-charged

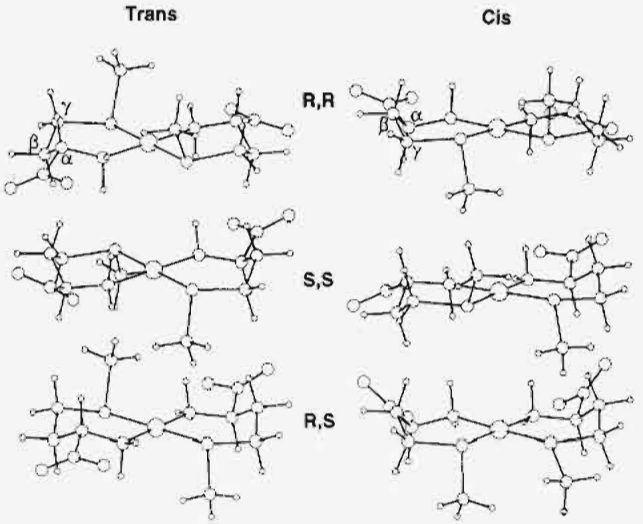

Figure 6. Energy-minimized structures of the diastereomers of *cis*-[Pt(L-Met-*S*,*N*)$_2$] and *trans*-[Pt(L-Met-*S*,*N*)$_2$]. These are consistent with the observed NMR $^3J(^1H-^1H)$ coupling constants. The change in chirality of sulfur from *R* to *S* changes the chelate ring conformation from an approximate envelope to a flattened boat, respectively.

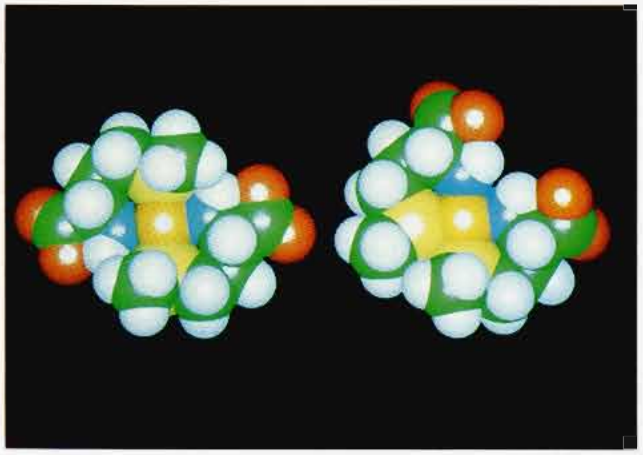

Figure 7. Space-filling model energy-minimized structures for *R*,*R*-*trans*-[Pt(L-Met-*S*,*N*)$_2$] (left) and *S*,*R*-*cis*-[Pt(L-Met-*S*,*N*)$_2$] (right). The colors for atoms are as follows: Pt, gold; C, green; H, white; N, blue; O, red, S, yellow. The more extensive hydrophobic face of the cis isomer can be seen.

S atoms and nearly neutral methyl and methylene groups opposite. In contrast to this, for the trans isomer there is an almost equivalent balancing of charges on opposite sides of the molecule. This is reflected in the difference in the dipole moments for the cis and trans isomers. The three cis diastereomers have dipole moments of 27.6, 29.4, and 29.1 D (*RR*, *RS*/*SR*, and *SS*, respectively, Table II) with the charge vector in the PtN_2S_2 plane, bisecting the S–Pt–S and N–Pt–N bonds and oriented from N to S. The three trans diastereomers have dipole moments of 8.7, 11.9, and 10.5 D (*RR*, *RS*/*SR*, *SS*, respectively, Table II), but now the charge vectors for the *RR* and *SS* diastereomers are perpendicular to the PtS_2N_2 plane and that for the *RS*/*SR* diastereomers points approximately along a Pt–S bond and is out of the plane by ca. 20°.

Discussion

[Pt(Met)$_2$] has been reported to be present in the urine of patients treated with the anticancer drug cisplatin, and was originally assigned a trans geometry.[3] Platinum–L-Met complexes have also been detected in blood plasma.[8,23,24] Recently we have prepared [Pt(L-Met)$_2$] by reacting either $[PtCl_4]^{2-}$, cisplatin, or

(23) Daley-Yates, P. T.; McBrien, D. C. H. *Biochem. Pharm.* **1983**, *32*, 181–184.

its diaqua complex with L-HMet in aqueous solution at neutral pH.[4] Methionine is an important amino acid in vivo, both inside and outside cells. The plasma concentration of HMet is ca. 35 μM, and may be higher in diseased states.[24] The amino acid may react directly with cisplatin or with its hydrolysis products, and the high trans influence of its thioether sulfur promotes labilization of the ammonia ligands.

^{195}Pt and ^{15}N NMR data have suggested that [Pt(Met)$_2$] consists of a mixture of cis and trans isomers, with the cis isomer predominating.[4] In the present work we have separated these isomers by reverse-phase HPLC. This has allowed us to characterize each isomer individually, and to study the isomerization process. There appear to be few previous reports of the kinetics of isomerization reactions of Pt(II) complexes in aqueous solution. Knowledge of the physicochemical properties of these isomers and the isomerization kinetics is likely to be of importance in understanding the excretion of platinum from the body.

Isolation and Characterization of Isomers. We achieved an efficient separation of the cis and trans isomers of [Pt(L-Met-*S*,*N*)$_2$], for example during reactions of [PtCl$_4^{2-}$] with L-HMet, using a reverse-phase C18 column with elution under mild conditions (H_2O and 95% H_2O/5% methanol as eluents). [PtCl$_4^{2-}$] is anionic and was eluted rapidly from the hydrophobic column. The neutral products were then eluted: first the trans isomer, followed by L-HMet, and then the cis isomer. The cis isomer has a more extensive hydrophobic face comprised of the β- and γCH$_2$ and *S*-CH$_3$ groups of the two chelated L-Met ligands (Figure 7), and would be expected to interact more strongly with the column. The cis:trans ratio at equilibrium determined by HPLC (87:13) is close to that we observed previously by ^{195}Pt NMR spectroscopy (89:11).[4] EHMO calculations confirmed that the cis isomer is more stable than the trans isomer.

Chromatographic separations of Pt(II)–L-Met complexes have been carried out by a number of groups previously using a variety of different procedures with adducts formed in vivo or in vitro. For example, Andrews et al.[7] found that 28% of cisplatin remained intact after 20 h of reaction with 1 mol of L-HMet when assayed by anion-exchange HPLC, with both mono- and bis-L-Met complexes present as products. They also monitored reactions by TLC using 20:1:5 2-propanol/formic acid/water (v/v). On reaction of cisplatin with 2 or 10 mol equiv of L-HMet, they detected only a single bis complex as product. Our multinuclear NMR studies have shown that 1:1 mixtures of cisplatin and L-HMet can contain a number of complexes including the bis complex, and 1:2 mixtures contain two separable complexes: the cis isomer, *cis*-[Pt(L-Met-*S*,*N*)$_2$] (87%) with lesser amounts of the corresponding trans analogue (13%). Therefore, chromatographic results have to be interpreted with care in view of the possible influences of eluents and column materials on the distributions of species.

We avoided the use of acetonitrile because it is a potential ligand for Pt(II)[25] and has been shown to react with hydrolysis products of cisplatin.[26] Riley et al.[21] found that at least six compounds were observed by HPLC (ODS Hypersil) when cisplatin–L-HMet mixtures were eluted with 12% acetonitrile. Although surfactants have often been used during separations of Pt(II) complexes by HPLC,[27] we avoided these too because we needed to isolate pure products.

We have previously used ^{195}Pt and ^{15}N NMR spectroscopy to characterize *cis*- and *trans*-[Pt(L-Met-*S*,*N*)$_2$] in mixtures of them resulting from reactions of [PtCl$_4^{2-}$] or cisplatin or its diaqua cation with either 1 or 2 mol equiv of L-HMet.[4] The cis isomer has a characteristic ^{15}N shift of ca. –21 ppm and $^1J(^{195}\text{Pt}-^{15}\text{N})$ of 265 Hz, compared to –40 ppm and 292 Hz for the trans isomer, in line with the well-known higher trans influence of S compared to N and consequent effects on shifts and couplings in square-planar Pt(II) complexes.[28]

One- and two-dimensional ^{1}H NMR spectra and 2D [^{1}H–^{15}N] NMR spectra for both *cis*- and *trans*-[Pt(L-Met-*S*,*N*)$_2$] are consistent with the existence of four inequivalent L-Met ligands for each isomer; for example there are four sets of αCH resonances, Table II. In work with [Pt(L-Met-*S*,*N*)Cl$_2$] we found that the conformation of the six-membered chelate ring was dependent on the chirality of coordinated sulfur.[4] Therefore it is reasonable to suppose that *RR-cis*-[Pt(L-Met-*S*,*N*)$_2$] and *SS-cis*-[Pt(L-Met-*S*,*N*)$_2$] each contributes one set of Met resonances with different shifts, and that *SR*- and *RS-cis*-[Pt(L-Met-*S*,*N*)$_2$] diastereomers (which are equivalent due to a C_2 symmetry axis) contribute two sets of resonances, one from the chelate ring containing *R*-sulfur and one from the *S*-sulfur ring. The areas of the resonances for the diastereomers are not equal and certain diastereomers must therefore be favored. For the cis isomer, S inversion is slow on the NMR time scale at ambient temperature, whereas the pronounced broadening of the ^{1}H NMR spectrum of the trans isomer suggests a faster inversion rate, as might be expected from the higher trans influence of S compared to N.[29]

The observed $^3J(^1\text{H}-^1\text{H})$ coupling constants (Table II) can be related to chelate ring conformations.[4] The large Hα–Hβ_a couplings (9.7 and 9.1 Hz) and small Hα–Hβ_b couplings (3.5 and 3.3 Hz) are consistent with an approximate envelope conformation for the six-membered chelate ring and an *R* configuration at sulfur. In contrast, Hα–Hβ_a coupling of 7.0 Hz and Hα–Hβ_b couplings of 4.0 and 3.3 Hz are assignable to a flattened boat conformation for the *S* diastereomer. Assuming a Karplus-type dependence, the values of $^3J(\text{NH}-\text{H}_\alpha)$ support these assignments: one large and one small value for an envelope conformation, and a medium and a small value for a flattened boat conformation (Table II). The analysis of the latter couplings was only possible with the use of 2D HMQC methods, Figure 4. The Hα–Hβ couplings for the trans diastereomers suggest that they have similar differences in chelate ring conformations, although in this case the individual NH couplings were not resolvable. The NH$_2$ ^{1}H NMR resonances are in a similar region of the spectrum to those of 1,2-diaminoethane Pt(II) complexes (unpublished work). It is notable that there is a significant difference between the shifts of protons on the same N atom in the cis complex (ca. 0.3 ppm) and that the resonances for the cis complex are shifted to higher frequency compared to those of the trans complex by ca. 0.2 ppm. The latter could arise from H-bonding between the two adjacent NH$_2$ groups in the cis isomer and solvent molecules.

Like the αCH ^{1}H NMR resonances, the ^{15}N peaks also occur in two pairs, showing that ^{15}N resonances are also sensitive to S chirality and ring conformation. The ^{15}N spectra for the trans diasteromers are not as well resolved, presumably due to exchange broadening.

The ^{1}H NMR spectrum of the equilibrium mixture of cis and trans isomers of [Pt(L-Met-*S*,*N*)$_2$] is particularly difficult to interpret without knowledge of the spectra of the separated isomers combined with their characterization by ^{15}N and ^{195}Pt NMR. Indeed Grochowski and Samochocka[30] have recently reported an incorrect assignment based on ^{1}H NMR spectra of mixtures alone.

The CD and UV spectra of the two geometrical isomers provide a rapid and convenient means for their identification and quantification, and may be useful in clinical analysis, Table III. The shift to lower energy of bands for the trans isomer compared to the cis isomer is consistent with the general trend observed for

(24) Norman, R. E.; Sadler, P. J. *Inorg. Chem.* **1988**, *27*, 3583–3587 and references therein.
(25) Fanizzi, F. P.; Intini, F. P.; Maresca, L.; Natile, G. *J. Chem. Soc., Dalton Trans.* **1990**, 199–202.
(26) De Waal, W. A. J.; Maessen, F. J. M. J.; Kraak, J. C. *J. Chromatogr.* **1987**, *407*, 253–272.
(27) De Waal, W. A. J.; Maessen, F. J. M. J.; Kraak, J. C. *J. Pharm. Biomed. Anal.* **1990**, *8*, 1–30.
(28) Pregosin, P. S. *Annu. Rep. NMR Spectrosc.* **1986**, *17*, 287–349.
(29) Cotton, F. A.; Wilkinson, G. *Advanced Inorganic Chemistry*, 5th ed.; Wiley Interscience: New York, 1988; p 1300.
(30) Grochowski, T.; Samochocka, K. *J. Chem. Soc., Dalton Trans.* **1992**, 1145–1149.

Table IV. Comparative Equilibrium and Kinetic Data for the Cis–Trans Isomerization of Pt(II) Complexes

complex	10^3k (s^{-1})	K^a	$\Delta H^\ddagger$ (kJ mol^{-1})	$\Delta S^\ddagger$ (J mol^{-1} K^{-1})	ΔH° (kJ mol^{-1})	ΔS° (J mol^{-1} K^{-1})	T (K)	solvent	ref
cis-[Pt(L-Met-*S*,*N*)$_2$]	(1.8 ± 0.1) × 10^{-2}		93 ± 5	−41 ± 16			296	H_2O	this work
trans-[Pt(L-Met-*S*,*N*)$_2$]	(1.2 ± 0.6) × 10^{-1}	6.7	95 ± 6	−18 ± 16	2 ± 11	23 ± 32	296	H_2O	this work
cis-[Pt(Et_2SO)$_2Cl_2$]	(5.2 ± 0.7) × 10^{-2}		44 ± 12	−152 ± 40			314	$CDCl_3$	12
trans-[Pt(Et_2SO)$_2Cl_2$]	(3.8 ± 0.1) × 10^{-1}	7.23	70 ± 6	−55 ± 21	26 ± 18	97 ± 61	314	$CDCl_3$	12
cis-[Pt(PEt_3)$_2$(CH_3)Cl]	9 × 10^{-3}	ca. 0[b]	101 ± 8	−9 ± 20	[c]		313	2-propanol	13
cis-[Pt(PEt_3)$_2$(CH_3)MeOH]$^+$	6.76	ca. 0[b]	106 ± 4	63 ± 12			303	methanol	14
cis-[Pt(PEt_3)$_2Cl_2$]		0.081			−10.3	−56	298	benzene	15

[a] $K = k_{tc}/k_{ct}$ = [cis]/[trans]. [b] Equilibrium lies well over to the trans side. [c] Data not available.

ligand-to-metal charge-transfer transitions of other Pt(II) complexes.[31] The lower energy bands (ca. 300 nm) are assignable to d–d transitions, and are readily resolvable in the CD spectrum, Figure 5.

Isomerization. The rates of interconversion of the isomers are very slow with half-lives of 22.4 h for the conversion of cis into trans and 3.2 h for the reverse isomerization (at 310 K). These rates are comparable with those reported for other square-planar Pt(II) complexes, Table IV, although there appear to be few other detailed studies of chelated complexes or isomerization reactions in water. One reported study is that of [Pt(Gly-*N*,*O*)$_2$], but this isomerizes thermally only in the presence of free glycine or photochemically. Detailed kinetic parameters were not reported for this system.[10]

For the majority of Pt(II) complexes, the trans isomer is the most thermodynamically stable, although there are cases where the cis isomer predominates, e.g. for L_2PtX_2 (where L = 1-alkyl-3,4-dimethylphosphole and X = Cl, Br, and I)[32] and [Pt(Et_2-SO)$_2Cl_2$], Table IV.[12] The isomerization rates for the latter complex are similar at comparable temperatures. In contrast, for both *cis*-[Pt(PEt_3)$_2$(CH_3)Cl] and *cis*-[Pt(PEt_3)$_2$(CH_3)-MeOH]$^+$ the trans isomer is highly thermodynamically favored.[13,14] The differences may be due to the presence of the two chelated ligands in [Pt(L-Met-*S*,*N*)$_2$], as opposed to monodentate ligands in [Pt(Et_2SO)$_2Cl_2$]. Also, different solvents were used in the study of these systems, and for [Pt(L-Met-*S*,*N*)$_2$] H-bonding with H_2O may play a significant role in the stabilization of the individual isomers. The cis isomer of [Pt(L-Met-*S*,*N*)$_2$] is entropy favored, suggesting that the solvent shell is more ordered for the trans isomer which has partial charges more evenly distributed throughout the molecule.

A number of mechanisms have been proposed previously for the isomerization of d^8 complexes.[16] In the consecutive displacement and pseudorotation mechanisms, a five-coordinate intermediate is formed by attack of the free ligand. Isomerization via a tetrahedral intermediate has also been proposed, but requires a relatively high energy intermediate with a triplet configuration.[33] The dissociative mechanism proceeds via a three-coordinate, T-shaped intermediate, which isomerizes and then reforms the four coordinate complex. We observed no change in isomerization rate on dilution of either *cis*- or *trans*-[Pt(L-Met-*S*,*N*)$_2$] suggesting that intermolecular interactions are not involved in the rate-limiting step. The high positive $\Delta H^\ddagger$ values and low values of $\Delta S^\ddagger$ suggest that the mechanism involves either a tetrahedral intermediate or chelate ring-opening and formation of a three-coordinate intermediate. We have observed ring-opening of *cis*-[Pt(L-Met-*S*,*N*)$_2$] at N by ^{15}N and ^{195}Pt NMR spectroscopy, but only at low pH in the presence of chloride ions.[4] Since we observed no change in the isomerization rate at pH 4 compared to pH 7, a mechanism involving a tetrahedral intermediate appears to be the most consistent with the present data. Scandola et al. proposed a twisting mechanism involving a pseudotetrahedral intermediate for the photochemically-induced isomerization of *cis*-[Pt(Gly-*N*,*O*)$_2$] to its trans isomer.[10]

It is interesting to note that during formation of [Pt(L-Met-*S*,*N*)$_2$] from $[PtCl_4]^{2-}$ and L-HMet, no trans isomer was observed in the initial stages. This suggests that the cis isomer is the kinetic product from this reaction and that an intermediate such as *trans*-[Pt(L-Met-*S*,*N*)(L-HMet-*S*)Cl] isomerizes rapidly before ring closure. Indeed, during NMR studies of this reaction we have observed only the cis isomer of this ring-opened complex and not the trans isomer.[4]

Conclusions

We have separated the cis and trans isomers of [Pt(L-Met-*S*,*N*)$_2$], a metabolite of the anticancer drug cisplatin, by reverse phase HPLC. These have been characterized by mass spectrometry and UV, CD, and 1D and 2D multinuclear NMR spectroscopy. The NMR data allow characterization of the three diastereomers for each geometrical isomer and suggest that chelate ring conformation is dependent on the chirality of the coordinated sulfur. In aqueous solution at neutral pH the isomers interconvert extremely slowly (half-lives of 22.4 h and 3.2 h for the cis and trans isomers, respectively, at 310 K) with the cis isomer predominating at equilibrium (K = 7.0). The mechanism of isomerization appears to involve a high-energy tetrahedral or three-coordinate intermediate. Extended Huckel molecular orbital calculations showed that the cis isomer was the more stable and revealed significant differences in the distribution of partial charges in the isomers. The cis isomer has a more extensive hydrophobic face, accounting for its slower elution from the hydrophobic C18 HPLC column, and this property may have implications for the partitioning of [Pt(L-Met-*S*,*N*)$_2$] in biological systems. It is now of interest to determine which isomer is preferentially transported through cell membranes and excreted from the body. If one isomer is preferentially excreted, then discovery of a catalyst for the isomerization could hasten the excretion of Pt from the body and lessen the toxic side effects of the drug.

Acknowledgment. We thank the MRC, the SERC, and the Wolfson Foundation for their support of this work and the Biomedical NMR Centres at Mill Hill (MRC) and Christopher Ingold Laboratories (University of London, Intercollegiate Research Service) for provision of NMR facilities. We also thank Dr. Alex Drake (ULIRS, Birkbeck) for CD spectra, the ULIRS (School of Pharmacy mass spectra service), Dr. Alan Tucker (Birkbeck) for assistance with computer graphics, Dr. Robert Deeth (Bath University) for advice on the implementation and interpretation of EHMO calculations, and Dr. U. Frey for helpful discussions of kinetic data. We are grateful to Dr. T. A. Frenkiel (Mill Hill) for help and advice with the HMQC experiments.

Supplementary Material Available: Figure D1, depicting the 400-MHz ^1H NMR spectrum of an equilibrium solution of [Pt(L-methionine-*S*,*N*)$_2$] (1 page). Ordering information is given on any current masthead page.

(31) Lever, A. B. P. *Inorganic Electronic Spectroscopy*, 2nd ed.; Elsevier: Amsterdam, 1984; pp 341–353.
(32) MacDougall, J.; Nelson, J. H.; Mathey, F. *Inorg. Chem.* **1982**, *21*, 2145–2153.
(33) Anderson, G. K.; Cross, R. J. *Chem. Soc. Rev.* **1980**, *9*, 185–215.